Production Engineering (2024) 18:779–785
https://doi.org/10.1007/s11740-024-01276-0

PROCESSES

Fundamental investigation on the time-variance of process stability

S. Jaquet[1] · A. Meijer[1] · J. Baumann[1] · D. Biermann[1]

Received: 17 November 2023 / Accepted: 15 March 2024 / Published online: 22 April 2024

Abstract
Disturbance factors, such as self-excited tool vibrations, limit the performance of modern machining processes and thus restrict the quality, productivity and sustainability of industrially manufactured components. The dynamic process stability is subjected to significant variances especially at the beginning of the tool life. To precisely quantify these variances, series of milling tests were conducted and analyzed using tools made of high speed steel (HSS) and cemented carbide for the machining of EN AW-7075. In all test series, a critical initial decrease of the stability limit was detected directly at the beginning of the tool life. In the following, a significant increase and subsequent almost constant stability limit was observed. In the case of the HSS cutters the achieved stability limit exceeded the initial level substantially. An increase in the process forces and flank wear was also measured over tool life but the progression cannot directly explain the extend and characteristics regarding the stability limit. The findings described have a considerable impact on the appropriate design of manufacturing processes and experiments to determine the dynamic stability of cutting operations.

Keywords Milling · Process dynamics · Chatter suppression · Flank wear

1 Introduction

The productive and economic efficiency of machining processes is determined by an increase of the material removal rate under the limiting boundary conditions of manufacturing accuracy and quality and is realized, for example, by an increase of the process parameters feed rate, cutting velocity and depth of cut [1]. Productivity is limited by disruptive effects in the milling process, such as tool wear or dynamic instability. The periodic engagement in the milling process as well as the resulting dynamic excitation can cause chatter vibrations [2], which drastically impair the production quality and the wear behavior of the tools, if the process parameters are not selected properly [3]. The avoidance of dynamic effects in the machining process is the subject of numerous research projects [4, 5]. Since long cantilevered and therefore flexible milling tools have to be used for milling deep cavities, the risk of dynamic disturbance effects, such as regenerative chatter, is comparatively high [6].

Unstable process conditions lead to an unfavorable wear development and an overload of the tool. Since the dynamic stability of a milling process depends not only on the cutting parameters, but also on the macroscopic and microscopic wear condition of the milling tool and thus changes over the time of use, these correlations are to be investigated in a time resolved approach. Only a detailed understanding of the wear-dependent application behavior of milling tools and its influence on the dynamic process stability enables an efficient process design.

Tool wear is associated with an increase of process damping which might have a stabilizing effect [7], which is based on the workpiece volume interacting with the flank face [8].

By applying an adjusted flank face chamfer, an increased process damping can be realized [9]. Due to the smaller clearance angles, an increased wear rate can be expected.

Several publications have found that flank wear—similar to an applied chamfer—is related to an increased process damping [10]. However, these investigations were limited to one wear state. In [7] this approach was extended to 3 conditions and a comparison of the experimental and simulated stability limits was carried out.

The objective of this study is to quantify the wear state at which cutting tools can be used with increased and constant

✉ S. Jaquet
simon.jaquet@tu-dortmund.de

1 Institute of Machining Technology, TU Dortmund University, Baroper Straße 303, 44277 Dortmund, Germany

Table 1 Tool geometry of HSS and carbide end mill

	HSS	Carbide
Diameter D	8 mm	8 mm
Number of teeth N_t	2	2
Rake angle Υ	11°	18°
Helix angle δ	30°	40°

process parameters. High speed steel (HSS) and cemented carbide tools were subjected to induce different wear rates during the experiments. The results obtained have significant implications for the optimal design of manufacturing processes in terms of tool life-dependent dynamic operating behavior.

2 Materials and methods

2.1 Materials

The workpiece material for the force measurement, the tool wear as well as the dynamic investigations was the Aluminium Alloy EN AW-7075. In order to compare different cutting tool materials with different wear rates, HSS and carbide end mills were tested (Table 1). The cantilever length was $l = 25$ mm, resulting in an aspect ratio of 3.125. With this ratio, significant differences in the stability limit could be shown over the tool life.

2.2 Experimental setup

The intention of the described investigation was to quantify tool life dependent variances with respect to the dynamic critical process stability and to evaluate correlations with the process forces and tool wear. The dynamic properties of the tool were determined by means of experimental modal analysis and can be assumed to be constant over the operation period. Considering the modelled dynamics stability diagrams were calculated applying a geometric physically-based milling simulation. Two process configurations were selected, comprising high and low process stability predictions, which were used to perform the force measurements and dynamic tests. Iteratively, a defined material volume was machined after which process force and flank wear measurements as well as dynamically critical machining test were conducted (Fig. 1).

The dynamically critical milling test was realized by programming a tool path with a linear increase of the radial depth of cut a_e, whereby the stability limit is exceeded and dynamic instabilities start to occur.

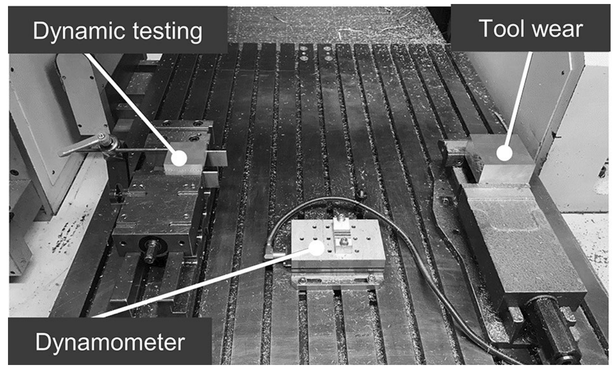

Fig. 1 Experimental setup for stability investigations

The axial depth of cut was $a_p = 3.5$ mm. A linearly increasing radial infeed of $a_{e,\,min} = 0$ mm up to $a_{e,\,max} = 8$ mm was used (Table 2). At the beginning of the iteration loops, a small amount of material was removed, since it was known from previous preliminary investigations that a large variance of the stability limit can occur in this range. For this purpose, a material removal of 35,000 mm^3 was taken in the first 4 iteration loops and 70,000 mm^3 thereafter. The termination criterion was defined as a stationary state in the stability limit.

To enable comparability of the tests, the same tool holder was used for all tests and a length tolerance of $\Delta l \leq 0.025$ mm was defined in order to keep the influence of the tool cantilever length on the dynamic properties and behavior constant. Moreover, a balance quality < 1 G was ensured.

The experiments were carried out on a Röders Tec RFM 1000 3-axis machine tool. After each tool wear iteration, the cutting forces were measured on the 9257B dynamometer from Kistler. Small and thus light specimen dimensions were used to not influence the natural frequencies of the dynamometer negatively with respect to the high tooth pass frequencies. The cutting forces were measured stationary in all 3 spatial directions and converted into the cutting force and the cutting normal force for further consideration (Fig. 2).

The acoustic measuring device Tascam DR-40 was used for in-process measurements. This data was used to determine the stability level and to compare the results with those of the optical analysis.

2.3 Design of a dynamically critical process

To determine dynamically critical operating points, the underlying modal parameters of a machining system must be determined. For this purpose, the frequency response function (FRF) of the tool was determined using

Table 2 Experimental design

Test	Cutting speed v_c in m/min	Depth of cut a_p in mm	Width of cut a_e in mm	Spindle speed n in 1/min	Feed per tooth f_z in mm
Cutting force	568; 693	3	1	22,600; 27,600	0.12
Dynamic test	426; 634	7	0–8	16,950; 25,250	0.12
Tool wear	568; 693	7	1	22,600; 27,600	0.12

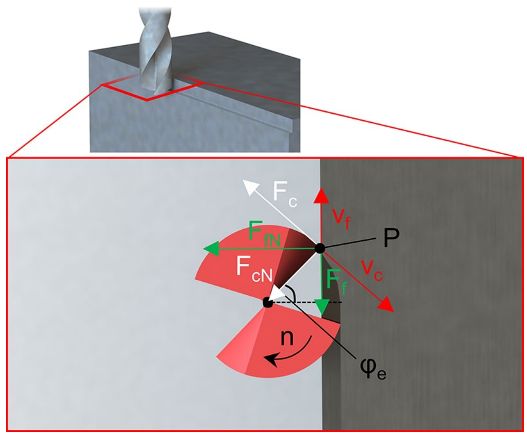

Fig. 2 Cutting force components measured with a dynamometer of the type Kistler 9257B

Table 3 Modal parameters XX of the FRF shown in Fig. 3

No.	$[f_0]$ = Hz	[m] = kg	$[\gamma] = s^{-1}$
1A	1061	0.284	207.842
2A	4967	0.039	728.456
3A	6983	0.062	470.444
4A	7333	0.009	887.713
5A	7766	0.039	327.208
6A	8163	0.073	1202.341
1B	1087	0.274	126.98
2B	1454	0.343	458.11
3B	1752	0.358	402.36
4B	3291	0.089	495.92
5B	4499	0.042	251.25
6B	4713	0.060	267.05

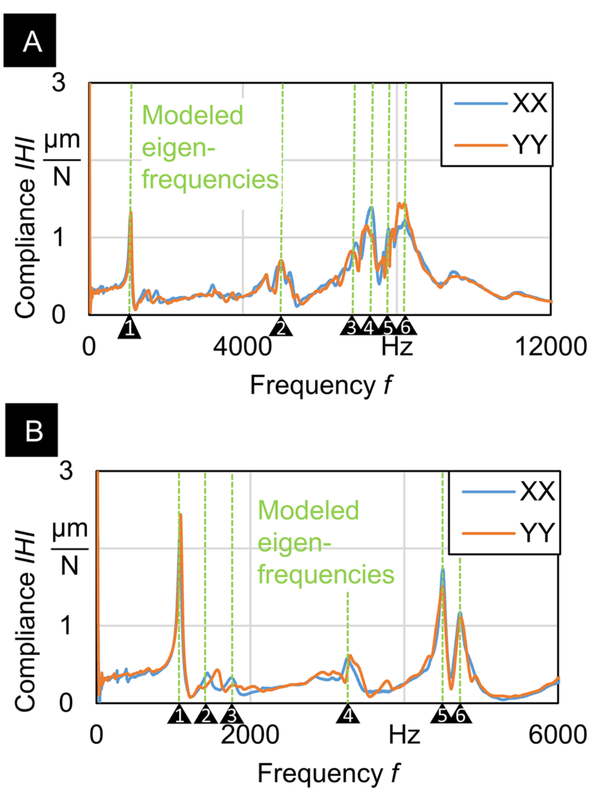

Fig. 3 FRF of HSS (**A**) and Carbide (**B**) milling tool

experimental modal analysis (Fig. 3). The system was excited using an impact hammer of the type 8206-002 by Brüel and Kjær, and the response was measured by an ultra-lightweight acceleration sensor (PCB Model 352C23).

The modal input parameters mass, stiffness and damping, which are necessary for the stability calculation, are then fitted using iterative optimization (Table 3).

The geometric physically-based process simulation [11] was applied with specifically calibrated models of cutting force and dynamics and typical process parameter values for the investigated application (Fig. 4). Based on the stability diagram, spindle speeds between $n_{min} = 16{,}950$ min^{-1} and $n_{max} = 27{,}600$ min^{-1} were selected, which comprise high and low process stability predictions. The selection of the operating points results in cutting speeds between $v_{c,min} \approx 426$ m/min and $v_{c,max} \approx 693$ m/min. The HSS and solid carbide tools were experimentally applied in dynamically critical milling processes with regard to the structure- and spindle speed-specific stability limit.

The machined workpiece surfaces were analyzed due to characteristic properties like chatter. In addition the acoustic emission during the experiment was evaluated in spectral analyses. Based on these measurements tool- and operation time-specific stability limits could be identified (Fig. 5). The spindle speed at $f_n = 460$ Hz and tooth engagement frequency $f_t = 920$ Hz are marked. When chatter marks start to occur, the amplitude increases in the frequency range of the first

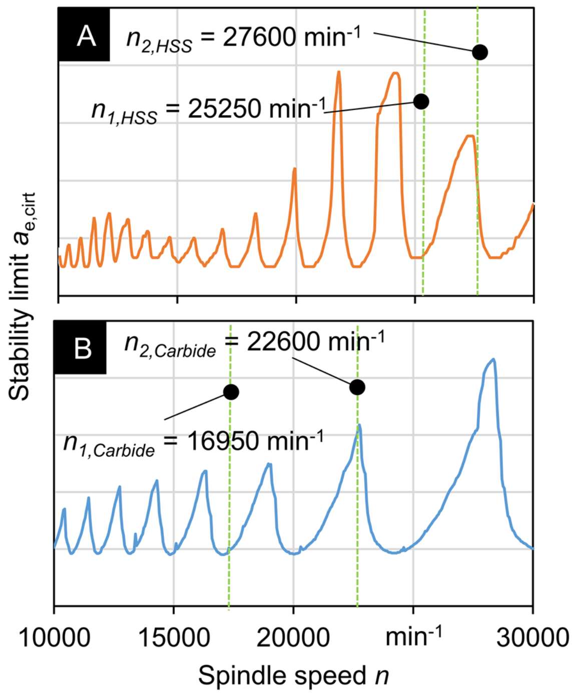

Fig. 4 Simulated stability diagram of HSS (**A**) and Carbide (**B**) tool

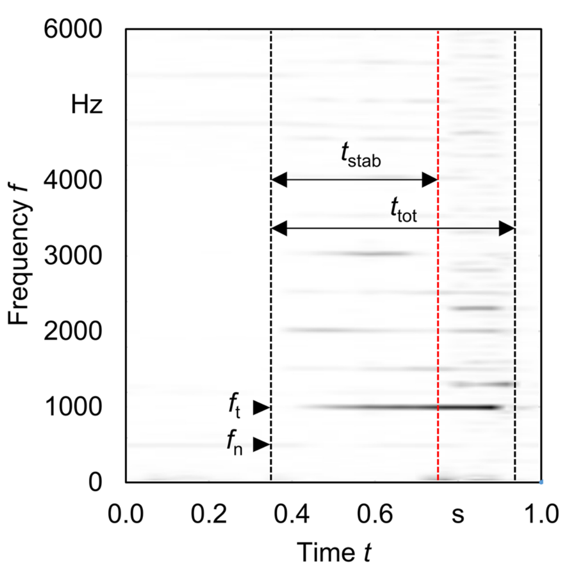

Fig. 5 Spectral analysis of the acoustic emission in situ of the HSS tool at $V_r = 210{,}000$ mm^3

natural frequency of the tool. Based on the maximum width of cut $a_{e,max}$ and the ratio of t_{stab} to t_{tot}, the critical width of cut $a_{e,crit}$ can be determined by the spectrogram. Here t_{stab} represents the process time up to the dynamically critical process point and t_{tot} the overall process time. By multiplying the ratio of these two values by $a_{e,max}$, $a_{e,crit}$ can be calculated due to the linearly increasing axial infeed.

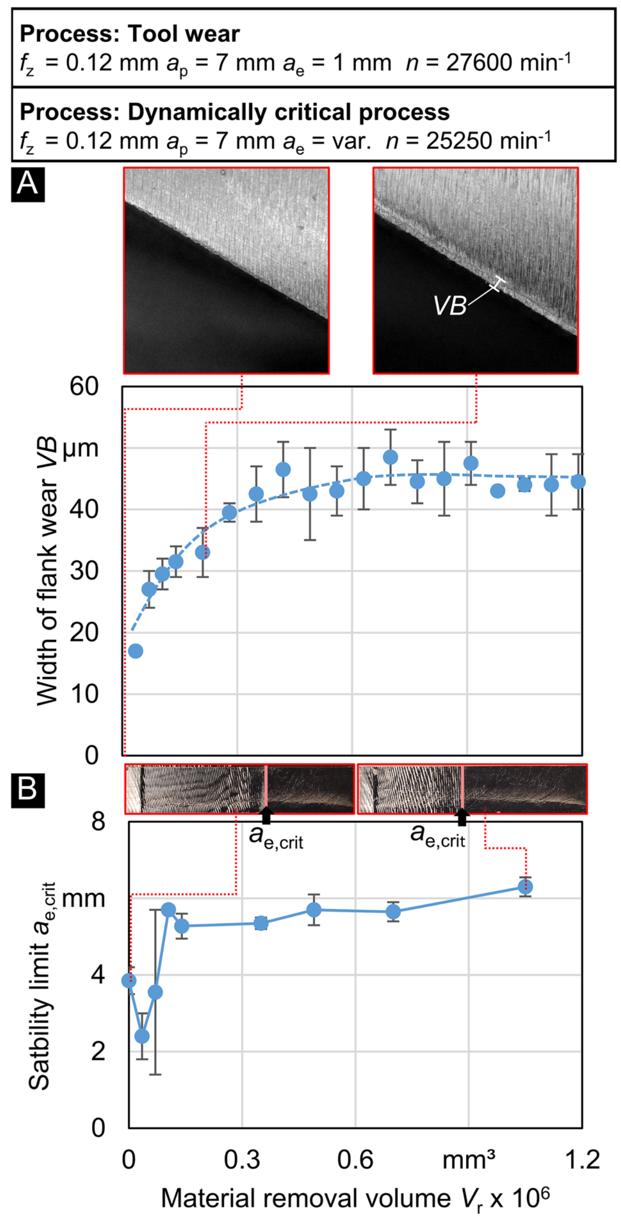

Fig. 6 Tool wear (**A**) and stability limits (**B**) over the material removal volume V_r using HSS tools

3 Results and discussion

3.1 Time-variant characteristics when using HSS cutters

Figure 6 shows the width of the flank wear and stability limit of the HSS tool over the tool life. The initial stability limit at $a_{e,crit} = 3.85$ mm is followed by a decrease to a value of $a_{e,crit} = 2.4$ mm after $V_r = 70{,}000$ mm^3. The stability limit exhibits an increased variance in this range. With further tool life, the limit increases above the initial stability limit to $a_{e,crit} = 5.7$ mm. Regarding the wear mark width VB at the circumferential cutting edge, an initial gradual increase can be observed. This converges in the further process at a value of $V_m = 45$ µm. A correlation between the progressions of wear mark widths and the stability limits is not evident.

The width of the flank wear represents the mean value of 2 tools used, each with 3 defined measuring points starting from the corner of the cutting edge (Fig. 7). In one of the tools used, a breakout of the cutting edge corner also occurred at the end of the tool life. The results of the stability test were therefore not considered in the last wear condition in order to exclude interactions on the process stability.

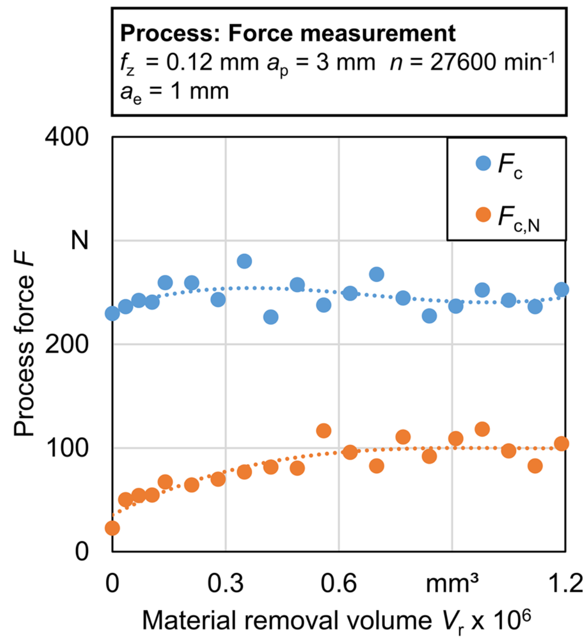

Fig. 8 Maximum process force F in dependency of the removed material volume of HSS cutter

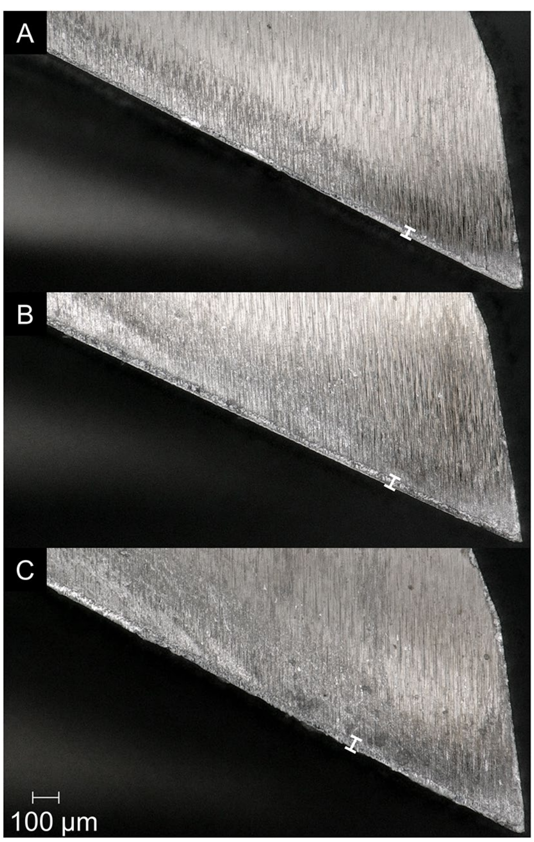

Fig. 7 Exemplary flank wear states at **A** $V_r = 140{,}000$ mm^3, **B** $V_r = 490{,}000$ mm^3 and **C** $V_r = 1{,}050{,}000$ mm^3

The process forces F_c and $F_{c,N}$ are shown over the tool life in (Fig. 8). The forces were evaluated at the same angle of rotation. The values shown are the averaged maximum values from several tooth engagements around the force maximum. The cutting force F_c increases from 229 to 264 N; an increase of 15%. The cutting normal force $F_{C,N}$ increases from 29 to 108 N is thus almost five times higher. Despite the increased deflection force, the stability limit of the process increases. Interdependencies between the process force, the width of flank wear and the stability limit therefore require more complex analytical approaches. The development of the flank wear and the cutting normal force are very similar. The stability limit is different. The high variances at the beginning of the tool life can neither be explained by the process force nor by the wear of the main cutting edge. A measurement of the microstructure, such as the cutting edge radius, could provide further information here.

3.2 Time-variant characteristics when using cemented carbide cutter

In Fig. 9, the wear mark widths and stability limits of the carbide cutting tools are presented. The tool wear investigations were carried out under dynamically stable operating conditions. The examination of process stability

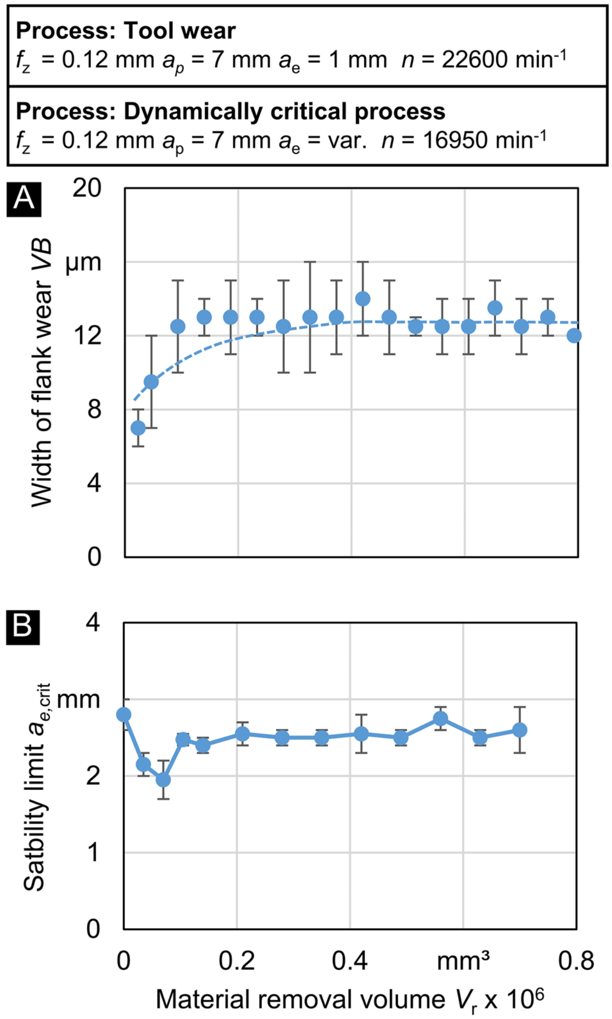

Fig. 9 Tool wear (**A**) and stability limits (**B**) over the material removal volume V_r using solid carbide tools

was conducted at a dynamically critical operating point with $n = 16{,}950\ \text{min}^{-1}$. Analogous to the HSS tools, an initial drop in the stability limit $a_{e,krit}$ can also be observed at $V_r = 70{,}000\ \text{mm}^3$. However, this value rises again, but unlike the HSS tools, does not exceed the value of the initially measured stability limit. In general, the stability level is lower compared to HSS, which might be explained by the lower inherent damping of the carbide compared to HSS. The increased wear resistance of the cemented carbide is evident in the wear mark width over the tool life. This initially increases continuously and then assumes an almost constant value at $VM = 12$ µm. The progression of the width of the flank wear also does not provide direct conclusions to be drawn about process stability. Compared to the HSS tools, the wear mark width is more homogeneously distributed over the circumferential cutting edge and no major breakouts were observed. The cutting volume was set to be smaller

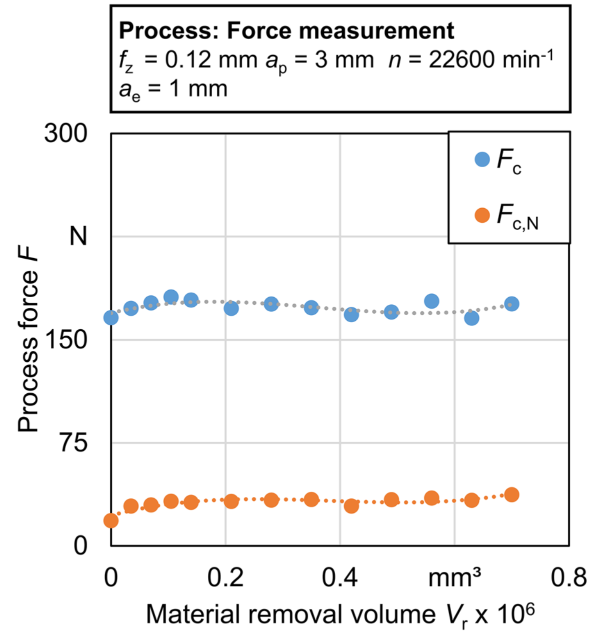

Fig. 10 Maximum process force in dependency of the material removal volume of cemented carbide cutter

compared to the HSS tools, as stationary cutting conditions were achieved faster.

Similarly, in Fig. 10 the force components F_c and $F_{c,N}$ over the tool life are depicted. In both force components, an initial increase is recognizable. Subsequently, both components settle at a nearly constant value. Compared to the results of the cutting normal force of the HSS tools, the values only slightly increase over the tool life. This can also be seen from the results of the wear mark width.

4 Summary and outlook

The presented work focused on the process stability of high-speed steel (HSS) and cemented carbide cutting tools, which was dependent on their tool life. A correlation between the width of the flank wear and the process forces on the dynamic behavior of the tools should be demonstrated. Therefore, workpiece material was removed iteratively, and the dynamic performance as well as the process forces and width of the flank wear were measured at discrete intervals.

The aluminum alloy EN AW-7075 was used as the workpiece material. Regarding the dynamic performance, a significant variance was observed especially at the beginning of the tool life for both cutting materials. The initial value of the stability limit was followed by a decrease to a minimum value. Later on, the stability limit of the cemented carbide tool reached the same level as that of the new tool, while the HSS tool even converged beyond the initial limit over time.

The width of the flank wear marks initially increased and then converged for both cutting materials. The different cutting materials showed a significantly different wear rate, resulting in increased wear marks for the HSS tools compared to the carbide tools. A similar trend was observed in the force components of the cutting force and the cutting normal force. While the cutting force remained almost constant over the tool life for both tools, the normal force of the HSS tool increased fivefold compared to the new tool.

However, a direct correlation between the dynamic performance and the wear marks and process forces could not be established. In conclusion, a more detailed analysis of the tool microstructure is required to explain the high variance in the dynamic behavior of milling tools at the beginning of their operation time.

Considering the findings described, it is urgently recommended that experimental investigations on process dynamics are always carried out with run-in tools. Otherwise overlapping effects have to be expected. This applies in particular if, for example, new process-stabilizing tool concepts or process strategies have to be evaluated.

Acknowledgements *Gefördert durch die Deutsche Forschungsgemeinschaft (DFG)—Projektnummer 426468684*. This research was funded by the German Research Foundation (DFG, Deutsche Forschungsgemeinschaft)—project number 426468684.

Funding Open Access funding enabled and organized by Projekt DEAL.

Declarations

Conflict of interest The authors declare that they have no conflict of interest.

References

1. Denkena B, Fleischer A, KG MDK (2016) Höchste Wirtschaftlichkeit bei der Aluminiumbearbeitung. Maschinenbau-Das schweizer Industriemagazin 5:18–22
2. Altintas Y, Ber AA (2001) Manufacturing automation: metal cutting mechanics, machine tool vibrations, and CNC design. Appl Mech Rev 54(5):B84–B84
3. Schmitz TL, Smith KS (2009) Machining dynamics. Springer, Cham, p 303
4. Zhu L, Liu C (2020) Recent progress of chatter prediction, detection and suppression in milling. Mech Syst Signal Process 143:106840
5. Munoa J, Beudaert X, Dombovari Z, Altintas Y, Budak E, Brecher C, Stepan G (2016) Chatter suppression techniques in metal cutting. CIRP Ann 65(2):785–808
6. Altan T, Lilly B, Yen YC (2001) Manufacturing of dies and molds. CIRP Ann 50(2):404–422
7. Denkena B, Krödel A, Relard A (2021) Using tool wear to increase process stability when milling Al7075 and AISI 4140+QT. Prod Eng 15(6):843–853
8. Wu DW (1988) Application of a comprehensive dynamic cutting force model to orthogonal wave-generating processes. Int J Mech Sci 30(8):581–600
9. Denkena B, Bickel W, Sellmeier V (2012) Flank milling of compliant workpieces with chamfered tools. Prod Eng 6:403–412
10. Altintas Y, Eynian M, Onozuka H (2008) Identification of dynamic cutting force coefficients and chatter stability with process damping. CIRP Ann 57(1):371–374
11. Wiederkehr P, Siebrecht T, Baumann J, Biermann D (2018) Point-based tool representations for modeling complex tool shapes and runout for the simulation of process forces and chatter vibrations. Adv Manuf 6:301–307